

Interdisciplinary design of a fish ramp using migration routes analysis

Gorazd Novak^{a,*}, Polona Pengal^b, Ana T. Silva^c, José M. Domínguez^d, Angelo Tafuni^e,
Matjaž Četina^a, Dušan Žagar^a

^a Faculty of Civil and Geodetic Engineering, University of Ljubljana, Slovenia

^b REVIVO Institute for ichthyological and ecological research, Dob, Slovenia

^c Norwegian Institute for Nature Research – NINA, Trondheim, Norway

^d EPHYSLAB Environmental Physics Laboratory, CIM-UVIGO, Universidade de Vigo, Ourense, Spain

^e School of Applied Engineering and Technology, New Jersey Institute of Technology, Newark, USA

ARTICLE INFO

Keywords:

Fishway
Ramp
River restoration
Smoothed particle hydrodynamics
DualSPHysics

ABSTRACT

The study presents several steps of a fish ramp geometry optimization performed with a 3D numerical model DualSPHysics, which is based on the smoothed particle hydrodynamics (SPH) method. The optimization process led to the design of a bottom ramp that is capable of providing suitable conditions for the migration of target fish species (*Salmo trutta*, *Phoxinus phoxinus*, *Cottus gobio*, and *Eudontomyzon vladykovi*). Migration routes were determined as complex 3D volumes of fluid according to the simulated velocity field in various steady flow conditions. Including three categories of potential migration zones (rest, effort, and limit zones), migration routes were quantified in high detail in terms of the size and position of each zone, and in terms of the distance from a given fluid part to the nearest rest zone. The interdisciplinary approach of this study also led to the development of new tools for the DualSPHysics model, specifically suited to improve functionality in eco-hydraulics research.

1. Introduction

1.1. Background

Drawing from the ecological niche concept (Grinnell, 1917; Hutchinson, 1957; Dingle and Alistair Drake, 2007), we recognize that each species is bound by its own set of limiting and optimum environmental conditions that define its behavior and survival. Although fish migration distances range from several hundred meters (short-distance migrants) to thousands of kilometers (long-distance migrants) (Aarestrup et al., 2009; Lucas et al., 2001), all fish move up and down the river during their life to fulfill the essential life processes (such as feeding, shelter, reproduction, etc.) (Jungwirth, 1998; Northcote, 1978; Lucas et al., 2001; Radinger and Wolter, 2014; Silva et al., 2018). Longitudinal connectivity is an essential function of rivers that not only enables the dispersal and migration of fauna (e.g. fish migration, macroinvertebrate dispersal, etc.) but also allows sediment transport, the key process in the creation of habitat diversity (Mikuš et al., 2021)

Across the globe, freshwater fish populations and biodiversity are in drastic decline. It is known that hydro-morphological alterations, especially barriers, are the most common pressure on surface waters in

Europe (EEA, 2018) and cause tremendous harm to the natural functioning of our riverine ecosystems (Chamberlain, 2020; European Environment Agency, 2020; Liermann et al., 2012; Silva et al., 2018; WWF, 2018), an indicator of which are fish populations (Deinet et al., 2020). More than one million barriers fragment European rivers (Belletti et al., 2020), of which more than 60,000 are impacting Slovenian rivers (Pengal et al., 2021).

Recent policies, such as EU Biodiversity Strategy (European Commission, 2020), the UN Decade on Restoration (UNEP and FAO, 2020), and the Green Deal (European Commission, 2019) call for a complete shift in our treatment of aquatic ecosystems from management and governance to stewardship and restoration.

As a mitigation measure, numerous fish passage solutions have been proposed, ranging from technical fish passes (pool passes, vertical slot passes - VSF, Denil passes, eel ladders, fish locks, fish lifts) to close-to-nature types (bottom ramps and slopes, bypass channels, fish ramps) (FAO and DVWK, 2002; Schmutz and Mielach, 2013; Mader et al., 1998)

However, recent findings suggest that common fishway design criteria do not adequately account for natural variation among individuals, populations, and species (Birnie-Gauvin et al., 2019; Silva et al., 2018). Engineered solutions often cannot reinstate the natural

* Corresponding author at: UL FGG, Hajdrihova 28, 1000 Ljubljana, Slovenia.
E-mail address: gorazd.novak@fgg.uni-lj.si (G. Novak).

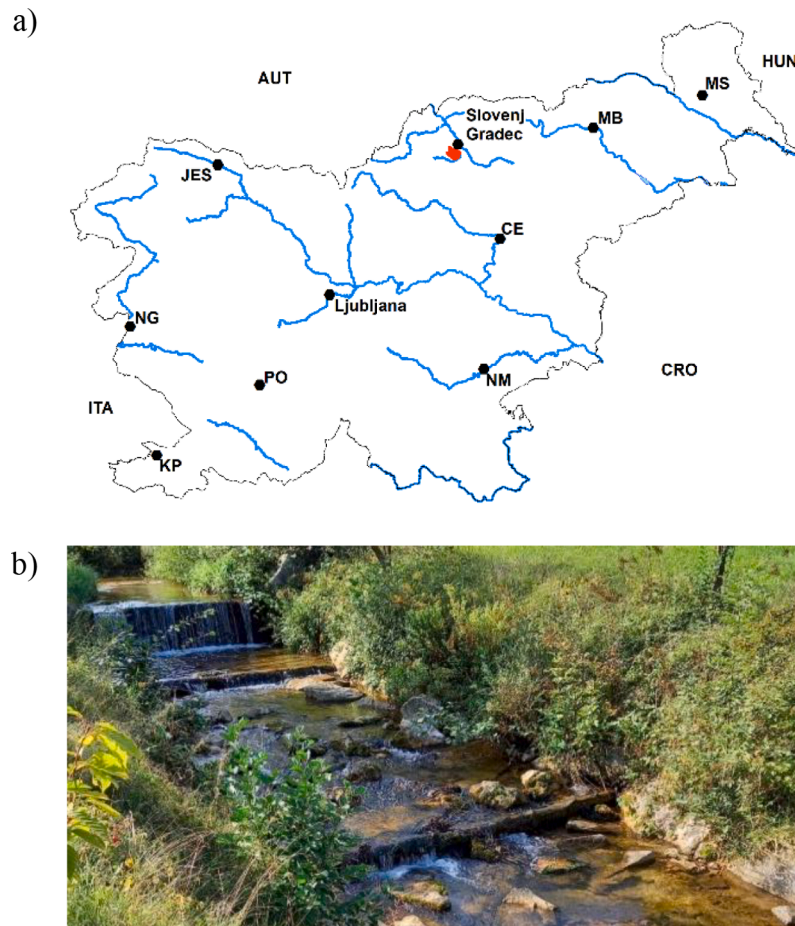


Fig. 1. The study area: a) location of the study site shown on a schematic map of Slovenia's rivers, b) photo of the present state of the weir and sills at the study site.

habitat and geomorphological properties of the river, and these objectives have been largely ignored (Birmie-Gauvin et al., 2019). Therefore, a shift from merely designing a hydraulic solution to providing a more ecological solution has been recognized as the most efficient approach (EEA European Environment Agency, 2018; IUCN, 2020; Raymond et al., 2017).

Among others, technical solutions to help fish migrate may include close-to-nature bottom ramps and by-passes. Such actions need to be carefully designed to determine their impact on the current state. This is where experience from experts in fish passage design, implementation, and monitoring is of great value.

One possible solution is also dam removal. Experts estimate that between 4000 and 5000 dams in total have already been removed in Europe, with records from France and Sweden indicating 2300 and 1600 dams removed, respectively (Gough et al., 2018). However, dam removal may also raise certain concerns (e.g. water surface and groundwater levels, erosion, and sedimentation), often leading to negative public opinion, especially where existing infrastructure and land use present limitations that cannot be avoided. Where a complete restoration of a river reach is not possible (e.g. a by-pass cannot be constructed due to existing land use constraints or economic reasons), partial removal of a dam or a weir, combined with additional mitigation measures, may present a viable compromise.

An example of such a compromise is the solution proposed in the present study, where the existing weir could be partially lowered (but not completely removed) and a suitable ramp could be implemented upstream and downstream of the weir, resembling the nearby natural stream channel.

Recently, the design of fish passes is increasingly based on 3D

modelling (e.g. Fuentes-Pérez et al., 2018 investigated turbulent flow in vertical slot fishways), detailed quantification (e.g. Marti-Puig et al., 2018 investigated animal scoring behavior in terms of trajectories), and integrating different aspects of habitat suitability (e.g. Shim et al., 2020 aimed to combine hydraulic and physiologic habitat suitability). The present study aims at providing an application of such an approach, including 3D modelling, detailed quantification of velocity fields and migration routes, and interdisciplinary cooperation.

Focusing on a real-life case of the Radušnica stream in Slovenia, the main goal of the study was to use computational fluid dynamics (CFD) to design a fish-friendly ramp that would provide nature-like flow conditions similar to those in a natural reach of an existing stream. As such, the present study provides designers and decision makers with a fish passage optimization CFD tool that takes into consideration both functionality and harmonious integration into the landscape.

One of the advantages of CFD is that it allows the quantification of flow characteristics that are difficult to measure either in a laboratory or in the field. As the present study involves a complex free-surface flow over a very non-uniform geometry, we adopt the fully three-dimensional (3D) DualSPHysics solver, which is based on the Smoothed Particle Hydrodynamics method (SPH), introduced by (Monaghan and Gingold, 1983).

Validated and verified against numerous benchmark tests (e.g. see spheric-sph.org and dual.sphphysics.org), the DualSPHysics has been successfully applied to cases of turbulent free-surface flow, such as in a weir-and-pool fishway (English et al., 2022), vertical slot fishway (Novak et al., 2019), and flow over a complex geometry bottom ramp (Novak et al., 2021). In the present study, new functionalities for eco-hydraulics applications were developed. New post-processing tools

Table 1
Characteristic cases (rectangular inflow, width $B = 4$ m for all cases).

case notation	inflow velocity u [m/s]	inflow depth h [m]	discharge Q [m ³ /s]
Q1	0.4	0.1	0.16
Q2	0.5	0.2	0.40
Q3	0.7	0.3	0.84

were added to the DualSPHysics, as explained in Section 2.3.

The driving hypothesis of the study was that the DualSPHysics software, supported by the newly developed tools, would allow a detailed design of a fish passage that takes into account the swimming capabilities of target species and flow characteristics in a geometrically and hydraulically complex environment. The design process involved several steps of geometry optimization. To quantify the proposed solution, potential migration routes were analyzed in terms of various zones and distances to their locations. Data on the swimming performance of local fish and lamprey species were used to identify different zones within the resulting velocity fields. Migration zones were treated as complex 3D volumes.

The main novelties of this study include: 1) the resulting velocity fields were analyzed in terms of potential migration routes represented by three different zones, i.e. rest, effort, and limit zone; 2) based on the velocity fields, the distances to nearest rest zones were calculated as a way of quantifying fish-friendliness to the proposed design; 3) DualSPHysics post-processing tools were improved to increase the code functionality in eco-hydraulics applications.

2. Methods

This study builds on our previous work (Novak et al., 2021), in which we first validated our numerical tools against the experiments by (Kupferschmidt and Zhu, 2017) and the numerical work by (Baki et al., 2020), and then modeled a bottom ramp fish passage. In the present study, this model was applied to design a nature-like fish ramp, which is in essence a similar task in terms of model performance (i.e. steady 3D water flow around and over obstacles of various shapes and sizes, with a focus on horizontal velocity fields), thus it is assumed the validation performed in our previous work is adequate for the present application. The optimization was an iterative process, starting from a very regular configuration and ending with a complex one that could be applied as a channel restoration measure for the actual site.

2.1. Study area

The study area is a short section of Radušnica, a 5 km long stream flowing into the Suhodolnica river in North-Eastern Slovenia (Fig. 1a). Radušnica is an interesting case study because it is quite typical for the region, but at the same time protected by Natura 2000 status. Even more importantly, local stakeholders have a positive attitude towards restoration plans, indicating that the conclusions of the present study (i.e., the proposed geometry of the ramp) could be implemented. At the target section, there is a 1.3 m high concrete obsolete weir that spans the entire 4 m width of the stream and is followed by several wooden sill cascades (Fig. 1b). The weir blocks migration of freshwater organisms, impacts sediment transport, and deteriorates the visual appearance of the stream.

Upstream of the weir, the natural channel has a minimum slope, while the average slope of the Radušnica is 1.5 %. The steep drop of the weir and the steps created by the downstream sills could be mitigated, for example, by keeping the weir but constructing a bottom ramp immediately downstream of the weir. Keeping the Radušnica's average slope of 1.5 %, the span of 1.3 m elevation difference would require a restoration of an 87 m section of the river channel, which could be achieved through re-meandering, but would require extensive land

purchases. Alternatively, the connectivity could be achieved by decreasing the elevation of the obsolete weir and restoring two shorter river sections upstream and downstream of the weir. In this study, one such section of the river channel (15 m length) is modeled as a typical case, considered representative of the flow dynamics in the entire restoration section.

As described in (Novak et al., 2021), no detailed hydrological data currently exists for the Radušnica, thus the input data for the model had to be estimated. In contrast to our previous study, where the inflow velocity was assigned as $u = 0.5$ m/s for all the cases, the present study considers wider range of conditions with inflow velocity ranging from $u = 0.4$ m/s to $u = 0.7$ m/s, inflow depths ranging from $h = 0.1$ m to $h = 0.3$ m, and inflow discharges ranging from $Q = 0.16$ m³/s to $Q = 0.84$ m³/s, as summarized in Table 1.

It was assumed that these cases correspond to typical discharges at the target location during different fish migration periods. Further work should include a more detailed field confirmation. The case denoted with Q1 represents dry conditions and its u and h correspond to data from the nearby Suhadolnica river ($u = 0.403$ m/s measured during low discharge). The case denoted with Q2 represents average conditions, while the case denoted with Q3 represents the highest flow during the fish migration period.

In its natural reach upstream of the weir, the Radušnica is a gently meandering 2 m wide channel with a pebbled bed and stones with diameters up to 0.25 m. In the model, these characteristics were taken into consideration during the geometry optimization and were modeled with various elements, as explained in Section 3.1.

2.2. The target species

Three species of fish and one species of lamprey live in the target stream: Brown trout (*Salmo trutta*), European minnow (*Phoxinus phoxinus*), European bullhead (*Cottus gobio*), and the Danubian brook lamprey (*Eudontomyzon vladkovi*). A range of approaches are used for estimating fish swimming capacities, e.g. sustained, critical, burst swimming speed, etc., defined in terms of speed and time sustained until fatigue (Table 2).

The Brown trout is the most efficient swimmer among the target species, with critical and optimal swimming speeds estimated at 65.4 cm/s and 31.6 cm/s, respectively (Tudorache et al., 2008). Bullhead anchor themselves with their pectoral fins at the bottom, so the critical swimming speed is practically impossible to determine (Tudorache et al., 2008). Therefore, only the maximum swimming speed was available from the literature, experimentally estimated at 112.5 cm/s (Tudorache et al., 2008). Because the ecological and biological requirements (especially in terms of biomechanics) of the other two target species have not been studied, selected proxies from ecologically similar species are used in the analysis. For the European minnow, the mean critical swimming speed of Spotfin shiner (*Cyprinella spiloptera*) was used, having a value of 60.8 cm/s (Nichols et al., 2018). The burst swimming speed of larval Pacific lamprey (*Lampetra tridentata*) ranges from 33.3 to 75.0 cm/s (Sutphin and Hueth, 2010), so the lower value was used to estimate the swimming capacity of the Danubian brook lamprey.

Data on the swimming speed of each target species as well as their ecological requirements (e.g. resting areas) was taken into consideration during the optimization of the channel geometry and for the definition of migration routes, as described in the results section. It was assumed that if a suitable migration route is achieved for the weakest swimmer, the species with higher capabilities would also find a suitable migration route, thus the optimization was based on the swimming capacities of the weakest swimmer, i.e. the Danubian brook lamprey. This means that the smallest parts of potential migration zones were defined as cylindrical volumes of water flow having the following characteristics: radius $r_m \geq 0.03$ m, length $l_m \geq 0.15$ m, and velocity magnitude $u_m \leq 0.45$ m/s (as explained in more detail in section 2.3.2).

Table 2

Swimming characteristics of the strongest (*Salmo trutta*) and the weakest (*Eudontomyzon vladykovi*) swimmer used in the analysis - all values are approximate, taken from the literature. Data on larval Pacific Lamprey was taken as a proxy for the Danubian brook lamprey.

species	body length [mm]	swimming mode	swimming speed [m/s]	time sustained [s]	distance swam [m]	reference data
<i>Lampetra tridentata</i>	72-143	sustained	0.45	33	15	Sutphin and Hueth, 2010
		burst	0.52	1	0,52	Sutphin and Hueth, 2010
<i>Salmo trutta</i>	78	critical	0.65	up to 1 h	2340	Tudorache et al., 2008
		maximum	≈ 5,5	1	5,5	Baudoin et al., 2015
		optimal	0.32	theoretically indefinitely	theoretically indefinitely	Tudorache et al., 2008

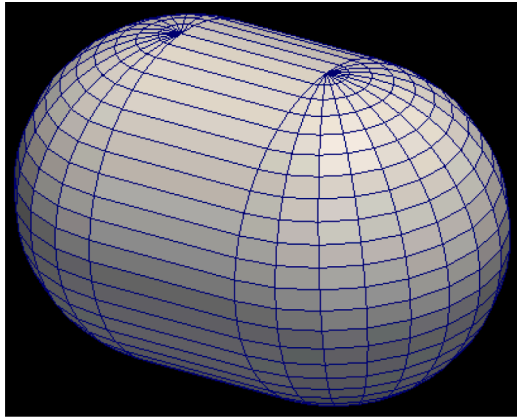


Fig. 2. Shape of an object that needs to fit in a resting zone.

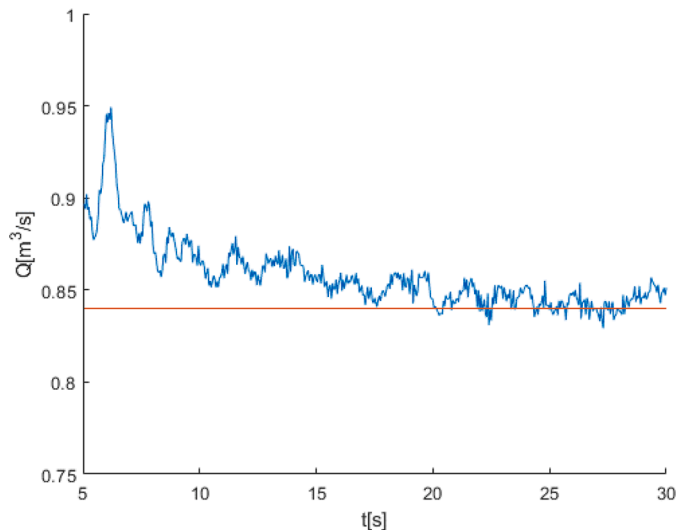


Fig. 3. Convergence of the flow for the Q3 case with optimized geometry.

Table 3

Optimization stages.

stage	parameter	values tested	selected variant
1	slope I [%]	$I = 1.5, 3, 4.5, 6, 7.5$ %	$I = 1.5$ %
2	bed roughness size (semi-spheres r_r) and number	$r_r = 0.02, 0.03, 0.04$ m; total: 0, 1300, 2600, 3900, 5200 elements	$r_r = 0.03$ m 3900 to 5200 elements
3	mean flow curvature (distance Δx_c between sets of larger obstacles)	$\Delta x_c = 2, 2.5, 3, 3.5, 4$ m	3.5 to 4 m, non-uniform
4	larger obstacles (cylinders with radius r_c , height h_c)	$r_c = 0.2$ m, $h_c = 0.15$ to 0.35 m	non-uniform
5	smaller obstacles (spheres with radius r_s)	$r_s = 0.07 - 0.15$ m	$r_s = 0.15$ m, non-uniform

2.3. Computational model

The numerical simulations in this study were performed using the DualSPHysics solver, a 3D open-source CFD model that is based on the SPH method, as described in (Domínguez et al., 2022). DualSPHysics is based on the weakly compressible formulation of SPH, and it can run on conventional CPUs or CUDA supported Graphics Processing Units (GPUs). The latter was employed in the present study and this allowed simulations with up to 8 million particles to be completed within reasonable computational times. The main features of DualSPHysics and the new features that were implemented in the present study are briefly reported below.

2.3.1. DualSPHysics

A detailed description of the DualSPHysics formulation can be found in (Domínguez et al., 2022), therefore only the formulations used in this study are mentioned here.

Modeling viscosity was achieved through an artificial diffusive term that is added to the momentum equation to reduce oscillations and stabilize the SPH scheme (Monaghan and Gingold, 1983). Due to its simplicity, the artificial viscosity formulation is often used as a physical viscous dissipation term with an associated coefficient α . Based on scaled flume experiments, the default value of this coefficient in DualSPHysics is $\alpha = 0.01$ (Altomare et al., 2015), and this value was used in the present study. Moreover, the use of a density diffusion term in the SPH method is necessary to reduce the density fluctuations associated with this method which can be aggravated in long-term simulations. The density diffusion term proposed by (Fourtakas et al., 2019) with the coefficient value of 0.1 was used to perform the simulations in this study.

In DualSPHysics, solid boundary conditions (e.g. for the riverbed and channel sides) can be modeled in two ways. Dynamic boundary conditions, DBC, are represented by fixed particles with density computed from the continuity equation and pressure obtained from the equation of state (Crespo et al., 2007). When using DBC, an unphysical gap between the fluid and the solid boundaries appears, lowering the accuracy of the pressure prediction at the boundaries. This can be alleviated by a second approach called modified dynamic boundary conditions, mDBC (English et al., 2022), with the density of boundary particles obtained from so-called ghost nodes, cleverly positioned within the fluid domain. In all simulations of the present study, the mDBC were employed.

In the present study, new tools were added to DualSPHysics to increase its functionality. Joined in a post-processing tool called FlowRest, these new options allow the calculation of 3D resting zones or migration routes and their distance to the main flow, as described in the following section.

2.3.2. FlowRest tool

A resting zone (or a migration zone) was defined as a volume of fluid where the flow conditions were likely to be suitable for the resting or migration of the target species (based on the biomechanic skills of each species). Thus, a resting/migration zone was defined as a 3D volume of fluid that simultaneously met the following two criteria: 1) the fluid velocity within the zone is below a specified value related to the swimming speed of the target species, i.e. $u \leq u_m$, and 2) the size (and shape) of the volume is larger than a specified value related to the size of

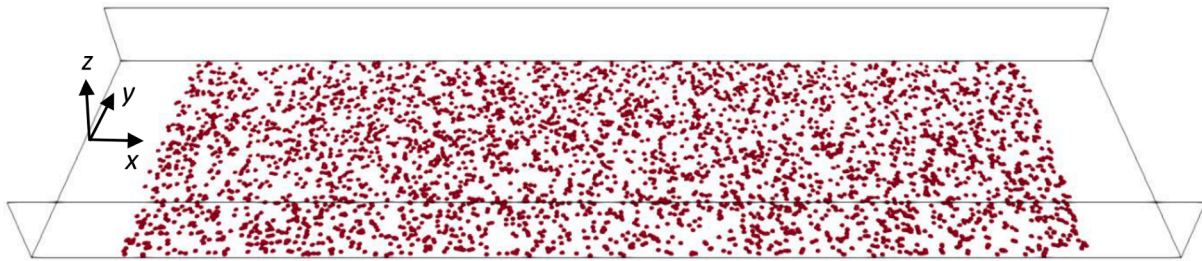


Fig. 4. Bed roughness elements – a variant with 300 elements per meter length.

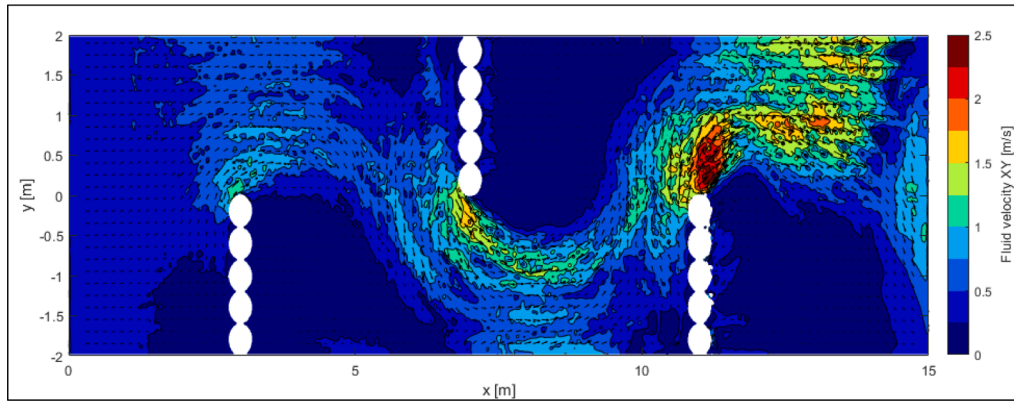


Fig. 5. Plan view of velocity fields [m/s] at $z = 0.05$ m plane, case Q2, optimization stage 3.

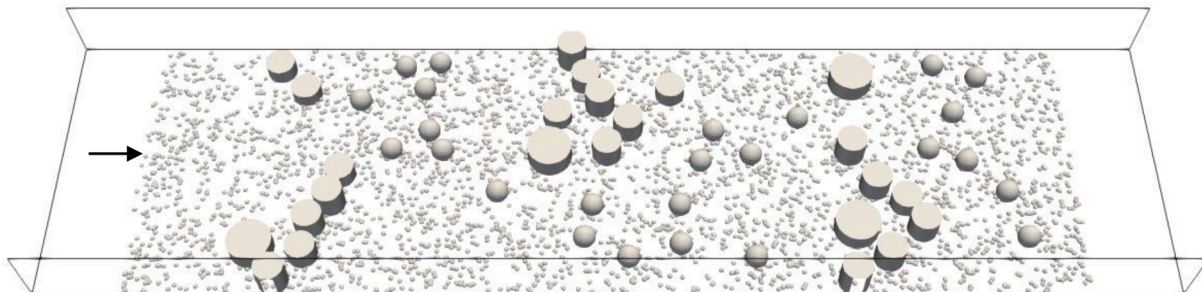


Fig. 6. Proposed geometry (a dry model; side view, arrow points downstream).

Table 4
Statistics of optimization stages.

stage	case	mean velocity [m/s]	slow fluid [%]	rest zone [%]
1	slope 1.5 %, smooth	0.33	13	8
2	slope 1.5 %, roughness 300/m'	0.31	21	16
3	as 2), and $\Delta x = 4$ m	0.20	45	43
4	as 3), and non-uniform distribution	0.25	39	36
5	proposed geometry	0.29	43	40

the target species, i.e. radius $r \geq r_m$ and length $l \geq l_m$. In other words, a pill-shaped object like the one shown in Fig. 2 must fit inside a resting/migration zone.

This way each zone can be identified computationally based on the simulation results (i.e. location of fluid particles and their velocity fields). Within post-processing, several characteristics of the zones were quantified, including their number, location, dimensions, volume (absolute and in percentage), and mean velocity within the volume. Next, a distance from any fluid point to the nearest rest zone was calculated and

again quantified in terms of mean and maximum distance. The main results of the FlowRest tool are summarized at the end of section 3.

2.3.3. Numerical setup

The model domain included an open rectangular channel with $L = 15$ m length, $B = 4$ m width, and $H = 1$ m height. The length of the domain was selected as a good compromise between computational cost and accuracy.

Various elements were added to the channel to mimic the stream substrate: randomly generated half-spheres for pebbles, suitably positioned spheres for stones, and cylinders representing rocks. In all the simulations the initial inter-particle distance was set to $dp = 1.5$ cm. Following the procedure described in (Tafuni et al., 2018), the constant slope of the channel was simulated via a horizontal channel subjected to an inclined gravity acceleration. For example, $I = 1.5$ % slope was modeled as a horizontal channel with $\vec{g} = (g_x, g_y, g_z) = (0.147, 0, -9.809)$ m²/s.

Steady flows at the inlet and outlet sections were imposed with constant fluid depths h and uniform fluid velocities u . Auxiliary upstream and downstream reaches of the channel, each 1 m long and located next to the inlet and outlet, respectively, were kept smooth and

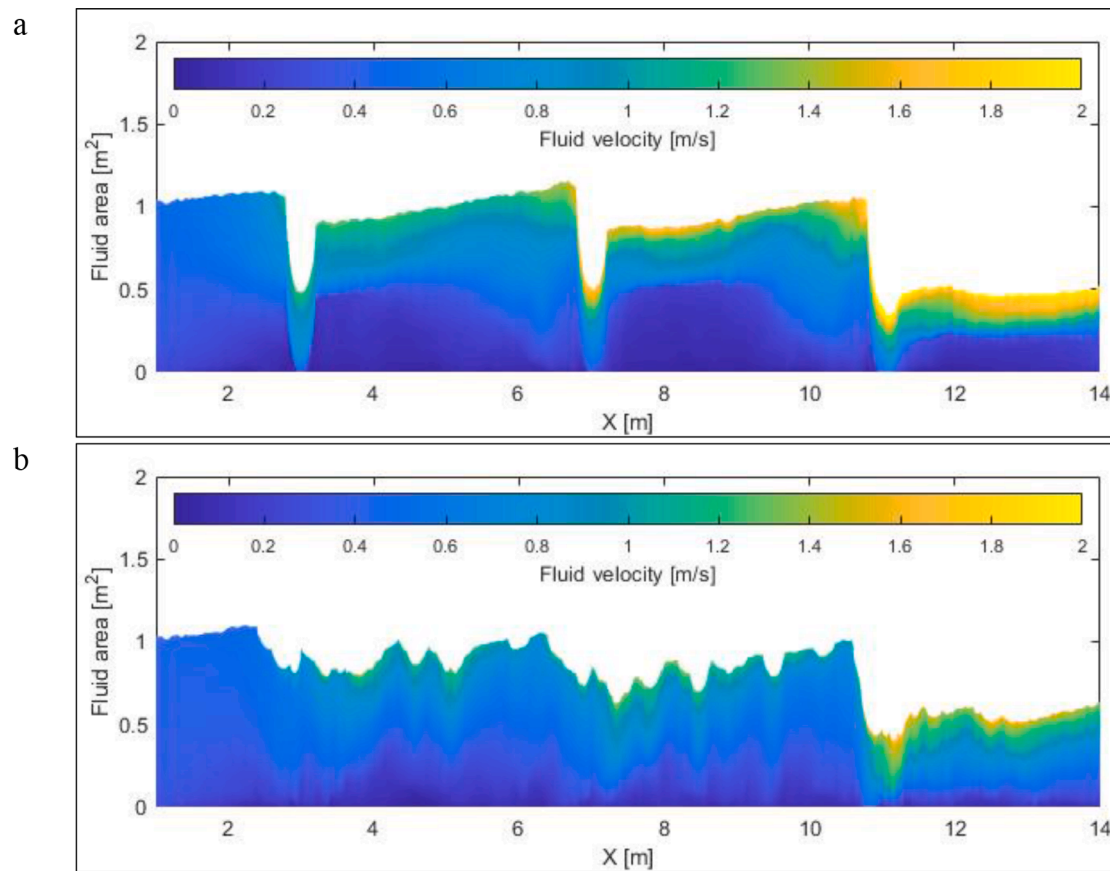


Fig. 7. Calculated area-velocity ratio for a 13 m long reach ($x = 1$ to 14 m) of the 15 m long domain ($x = 0$ to 15 m): a) uniformly curved stream (stage 3 variants), b) proposed geometry.

without any obstacles. With the initial fluid depth and velocity set to desired values, the main simulations covered 30 seconds of physical time, so that steady conditions were accomplished.

The convergence of the flow can be analyzed in terms of the discharge calculated volumetrically from the fluid particles (i.e. as a volume of fluid divided by time). For the Q3 discharge ($Q = 0.84 \text{ m}^3/\text{s}$) flowing over the proposed geometry, the convergence was confirmed with the following result (Fig. 3; a horizontal line showing $Q = 0.84 \text{ m}^3/\text{s}$ is added for easier visualization):

Note that the first 5 seconds of the simulation are not shown and that it takes some time for the initial condition to evolve according to the ramp characteristics. Fig. 3 shows that convergence occurred after 20 seconds. As mentioned, our simulations of the proposed configuration extended over that period.

3. Results

3.1. Geometry optimization

The proposed design of the presented nature-like channel was obtained as the result of several optimization stages, going from a simple uniform geometry to a complex one. The main optimization criteria were velocity fields, especially near the bed and in the mid-depth region.

These stages investigated the effect of the following parameters: 1) channel slope, 2) bed roughness, 3) curvature of the mean flow, 4) position and size of larger obstacles, 5) position and size of smaller obstacles against the swimming capacities of the target fish and lamprey. The main steps are summarized in Table 3. Each stage represents an intermediate step toward the final solution and is thus described only briefly, while the final geometry is described in more detail.

The process was completed iteratively, considering the comments by

engineers and biologists in our team. The best configuration from the first stage was fixed in the second, then the best option from the first two stages was fixed in the third, and so on. All optimization stages were performed using input data u and h for the Q2 case, which represented the average discharge.

3.1.1. Bed slope

Stage 1 investigated the slope I of a smooth channel and confirmed I should be kept as low as possible. With the inlet imposed the same way as the outlet ($u_{in} = u_{out}$, $h_{in} = h_{out}$), a hydraulic jump occurred in cases with a steeper slope. Maximum velocities occurred upstream of the hydraulic jump, ranging from 2.0 to 4.5 m/s for $I = 1.5\%$ to $I = 7.5\%$, respectively.

3.1.2. Bed roughness elements

Stage 2 employed $I = 1.5\%$ slope in all the cases and showed that the bed roughness elements decreased the near-bed velocities and slightly increased the fluid depth without affecting other overall characteristics of the flow. Model roughness represented by semi-spheres $r_r = 0.03 \text{ m}$ was selected as the best approximation of the bed along the natural part of the Radušnica. The bed roughness elements were generated along the width B and from $x = 1 \text{ m}$ to $x = 14 \text{ m}$ and were randomly placed to obtain a more natural (non-uniform) distribution. An example is shown in Fig. 4.

Model variants ranged from a case of a smooth bed (i.e. zero bed roughness elements) to a case with 5200 semi-spheres (i.e. an average of 400 elements per meter length). Based on the resulting velocity fields for the $z = 0.05 \text{ m}$ plane parallel to the bed, a configuration with 3900 elements (i.e. 300 elements per meter length) was selected.

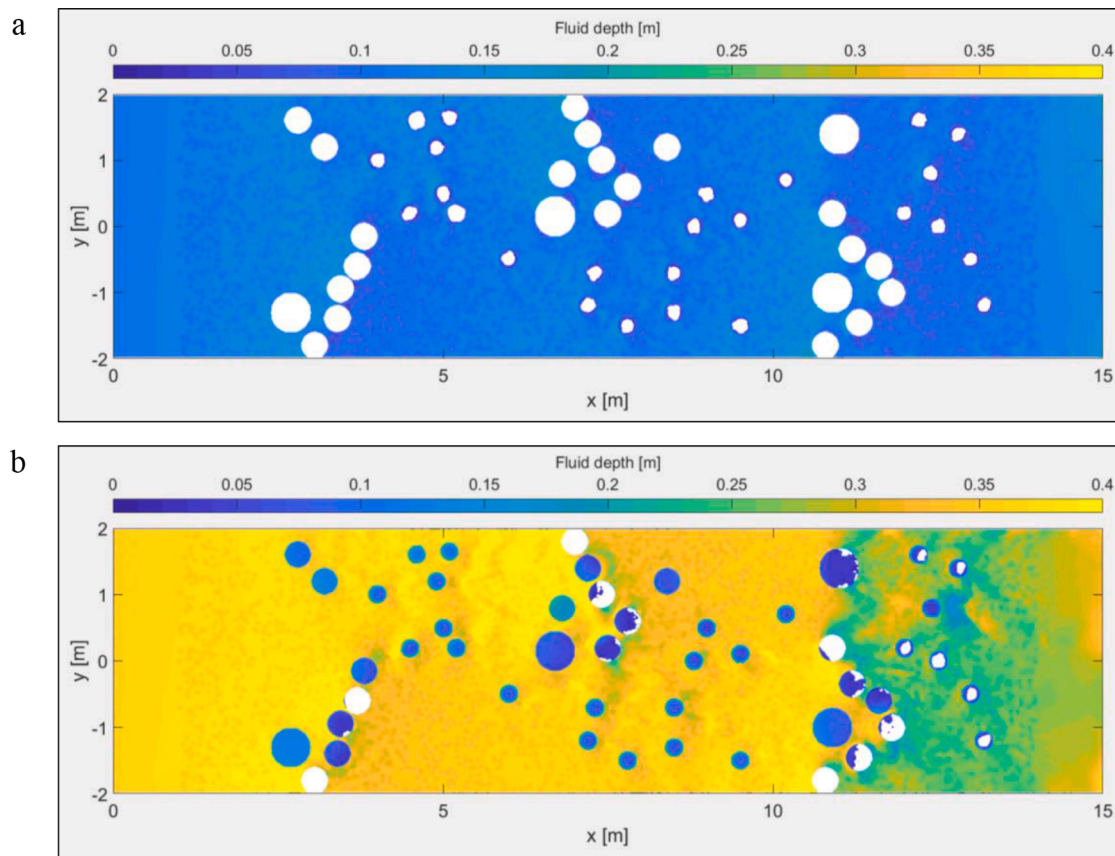


Fig. 8. Plan view of flow depth [m]: (a) case Q1, (b) case Q3.

3.1.3. Mean flow curvature

In stage 3, the $I = 1.5\%$ channel with a total of 3900 bed roughness elements was equipped with transverse sets of five equal cylinders with $r_c = 0.2$ m, $h_c = 0.3$ m. Uniformly distributed at a longitudinal distance Δx_c apart, their purpose was to replicate the meandering of natural streams (somewhat resembling technical types of fishways) and diversification of flows. Based on the resulting velocity fields, the geometry with $\Delta x_c = 3.5$ to 4 m was selected as the best option (Fig. 5):

Note that in Fig. 5 the velocities at the downstream line of obstacles locally reach above 2 m/s even at Q2 and even close to the bed. The figure shows a flow that is steady (i.e. not changing with time) and non-uniform (i.e. changing with location); even in equally wide sections of unobstructed flow the velocity fields change with location.

3.1.4. Size and position of larger obstacles

In stage 4, larger obstacles were placed transversely but included cylinders of various heights and radii. The following variants were tested: a) $r_c = 0.2$ m, $h_c = 0.3$ m (horizontal high crest), b) $r_c = 0.2$ m, $h_c = 0.15$ m (horizontal low crest), c) $r_c = 0.2$ m, $h_c = 0.15$ to 0.35 m (stepped crest; h_c decreasing towards the channel axis), d) $r_c = 0.2$ m, $h_c = 0.15$ to 0.35 m (distributed non-uniformly, variant 1), e) $r_c = 0.2$ m, $h_c = 0.15$ to 0.35 m (distributed non-uniformly, variant 2).

Based on the resulting velocity fields, the last variant was selected.

3.1.5. Size and position of smaller obstacles

In stage 5, sets of larger obstacles were changed so that each set included more cylinders with their size and position varying even more than in stage 4. Additionally, smaller obstacles (i.e. spheres) were added within the main flow region. The cylinders and spheres were added in several steps, iteratively providing a greater variety of velocity fields while simultaneously decreasing the maximum velocities to establish suitable conditions for all target species. The optimization resulted in

the final geometry of a nature-like channel, shown in Fig. 6.

Fig. 6 shows bed roughness elements (a total of 3900 semi-spheres with $r_r = 0.03$ m, distributed along the 13 m reach), three sets of eight larger obstacles (cylinders with $r_c = 0.2$ to 0.3 m and $h_c = 0.2$ to 0.45 m), and twenty-five smaller obstacles (spheres with radius $r_s = 0.15$ m). This geometry was later used with Q1 and Q3 flow conditions, as those two cases were estimated as being the most potentially problematic in terms of low depth (Q1) and high velocities (Q3). Thus, the main results presented next focus only on Q1 and Q3 conditions.

3.1.6. Statistical comparison of optimization stages

Typical cases of optimization stages are compared in terms of statistics given in Table 4.

In Table 4, the notion of slow fluid means the volume of fluid where $u < 0.5$ m/s, while a rest zone is defined as having a mean $u < 0.45$ m/s, which corresponds to the effort migration zone, discussed in section 3.4.

Interestingly, the variant representing stage 3 seems to be the best, according to the selected statistics. However, the apparent superiority of the stage 3 configurations is misleading. Flow in all of the stage 3 variants is a uniformly meandering stream with high velocities in the narrow sections and low velocities behind obstacles. This can lead to a favorable average, but such a geometry is inferior to the one proposed in the present study because the latter allows various paths of migration.

In our previous work (Novak et al., 2021), a tool for the calculation of the ratio between the flow area and flow velocity was introduced. Applied to each cross section of the model, this tool gives a clearer view of flow characteristics than most common statistics. A comparison of a typical uniformly meandering stream (stage 3) and the proposed configuration is presented in Fig. 7.

Fig. 7a shows distinctive dents at locations of narrow sections; at these locations the flow depths are lower and the velocities are higher, making these parts more difficult for a fish to pass. In contrast, Fig. 7b

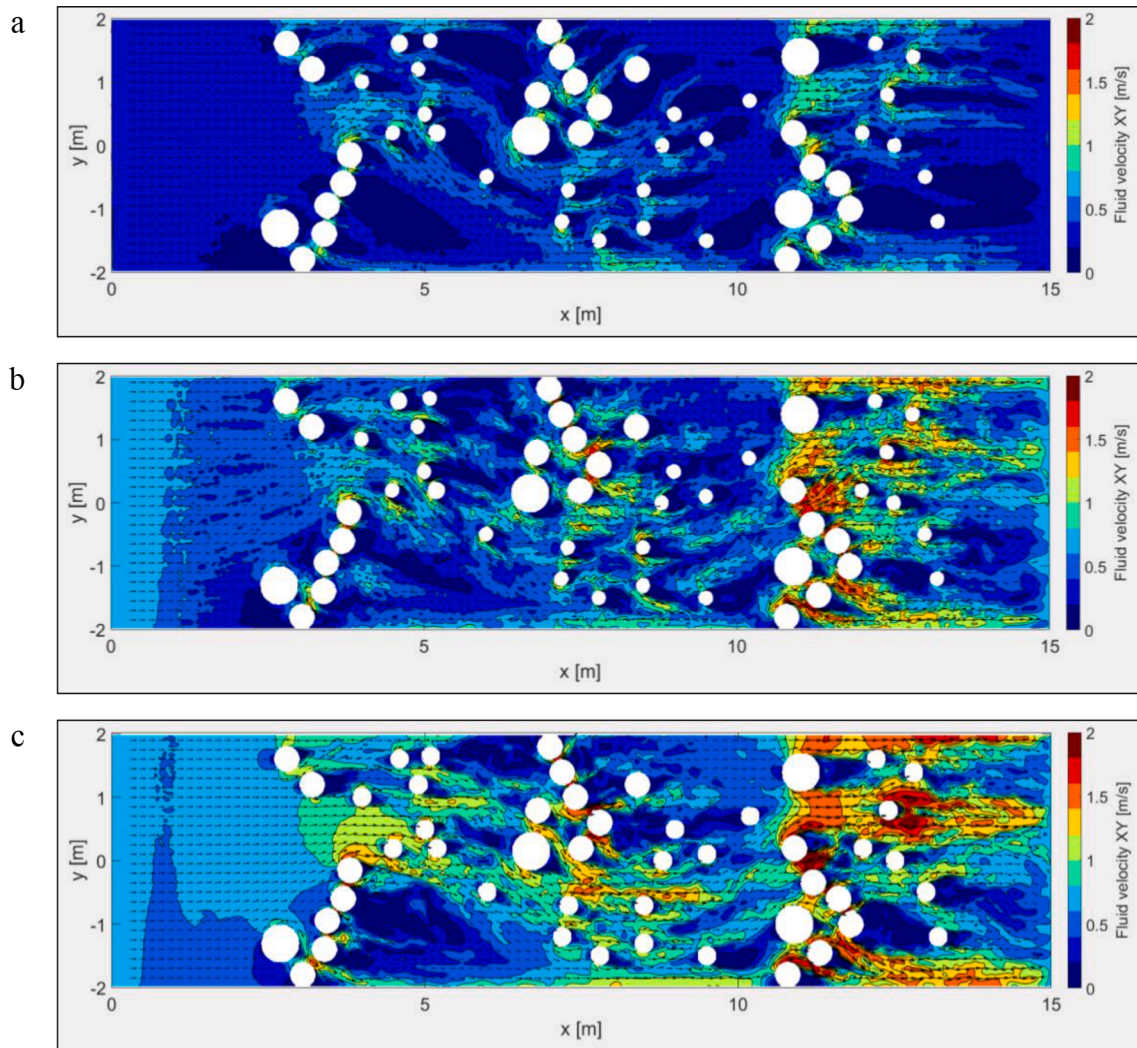


Fig. 9. Plan view of velocity fields [m/s]: a) $z = 0.05$ m plane, case Q1, b) $z = 0.05$ m plane, case Q3, c) $z = 0.15$ m plane, case Q3 (z is a distance above the channel bed).

Table 5
Types of zones forming a migration route.

zone type	velocity range [m/s]	required effort	representation (Figs. 10 and 11)
rest	0 – 0.34	can rest	green
effort	0.34 – 0.45	can maintain for a certain time	yellow
limit	0.45 – 0.52	can maintain for a few seconds	red

shows a much more gradually varying flow with a slightly smaller portion of very low velocities, but also with a distinctly smaller portion of high velocities – making such fish pass more efficient.

3.2. Flow depth

The first critical parameter defining suitable fish migration routes is the flow depth (Baudoin et al., 2015). The results for the Q1 (dry conditions) and the Q3 (larger discharge) cases are shown in Fig. 8a and 8b, respectively. Note that Fig. 8 shows the fluid depth above the solid boundary (bed, roughness element, smaller or larger obstacle), not the water surface elevation.

The proposed geometry provides a depth of about 0.1 m in dry

conditions (Fig. 8a) and a relatively uniform depth of about 0.3 m during the larger discharge (Fig. 8b).

3.3. Velocity fields

Velocity was the second critical parameter that was analyzed and used to define the potential routes for fish migration. In the presented model, all three velocity components (longitudinal u , transverse v , vertical w) were calculated for each location (x, y, z) of the domain, and for each output step (outputs for every 0.05 s of the simulation were selected). It was decided to focus on velocity fields at the end of the simulation, given as vector fields in planes, located at a constant z above the channel bed. Such slices of complex 3D fields are presented in Fig. 9, including near-bed velocities ($z = 0.05$ m plane) and mid-depth velocities ($z = 0.15$ m plane).

Fig. 9a shows that in dry conditions (case Q1) velocities remain mostly below 0.5 m/s with numerous areas of very low velocities (< 0.2 m/s). Fig. 9b shows how near-bed velocities increase with discharge. Velocities of up to 1.5 m/s occur in separate jets within the downstream set of rocks, but these conditions are localized. Figure 9c confirms that mid-depth velocities are greater than the near-bed ones. Local maximum values reach 2 m/s, but there are areas of low velocities (< 0.4 m/s) nearby.

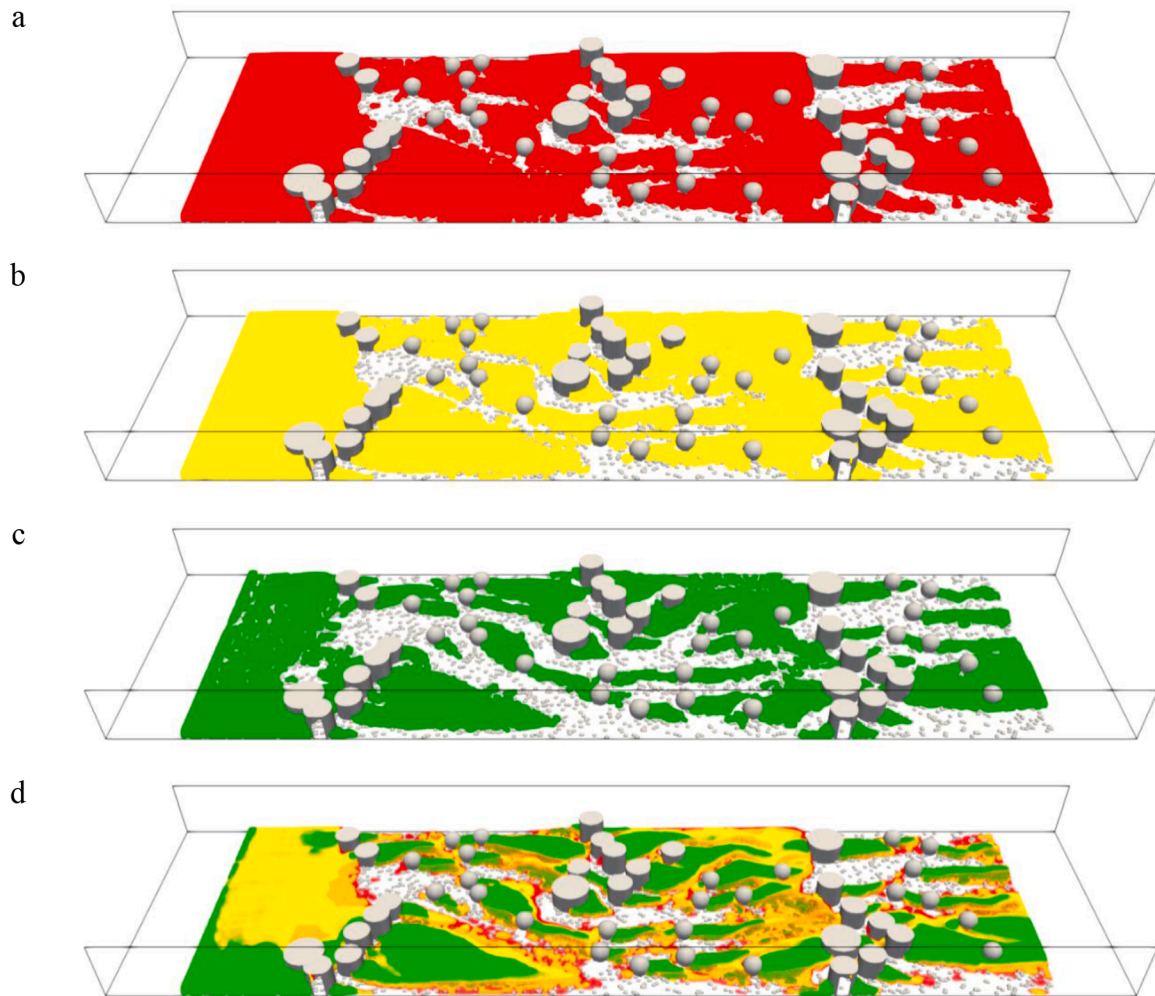


Fig. 10. Side view of migration zones with diameter $d \geq 0.03$ m, length $l \geq 0.15$ m for the Q1 case: (a) limit zones, (b) effort zones, (c) rest zones, (d) all zones with some transparency of colors to show the transition between the zones.

3.4. Migration routes

Since fish migration is essentially limited by the swimming capacities of each species, we define migration routes as the paths in which flow conditions correspond to the swimming capacities of the fish and, as such, theoretically allow fish to move along the river. Such routes consist of migration zones, as defined in section 2.3. A migration zone can be regarded as a volume of fluid with a certain velocity, radius, and length. In our case, the following values were selected: radius of at least $r_m = 0.03$ m, length of at least $l_m = 0.15$ m, and velocity thresholds ranging from $u_m = 0.34$ m/s to 0.45 m/s to 0.52 m/s. These velocities can be used to define different types of zones, as listed in Table 5.

All three zone types combined represent a migration route. The listed values correspond to experimental results for optimal, sustained, and critical/burst swimming speeds for target fish. These zones are 3D volumes that form complex shapes, not just layers limited to the water surface. Migration zones for Q1 and Q3 cases are given in Figs. 10 and 11 respectively.

Figs. 10 and 11 show that lower velocity volumes are located behind various obstacles and that the extent of limit zones is expectedly larger than the extent of the rest zones. In the Q1 case, migration routes are almost continuous, while in the Q3 case they are smaller and more fragmented.

Besides the size and position, the present study introduces also the calculation of the distance between the migration zones. Applying the proposed geometry, they are readily reachable from practically any

location, as confirmed in Fig. 12, which shows a map of the distances from fluid points to the nearest migration zone (selected here for the comparison are effort zones with $u_m \leq 0.45$).

In Fig. 12, the main flow region (lighter) and the low-velocity regions (darker) can be distinguished. Note that larger distances appear only close to inlet and outlet sections, which are on the edge of the designed channel reach. Within the reach with obstacles, the distances to the nearest migration zones are below 0.5 m and 1.5 m in the Q1 and Q3 cases, respectively. Some main statistical characteristics of the migration zones are summarized in Table 6.

Table 6 shows that, during low discharge, the percentage of migration routes is larger due to the lower flow velocities. Also, the volumes of zones increase if we allow a larger velocity threshold.

4. Discussion

Based on flow depth results (Fig. 8), the proposed geometry provides sufficiently deep flow even in dry conditions. Important advantages of the proposed geometry are its bed roughness elements and obstacles (model stones and rocks) of various heights which allow water to flow around or over them, providing target species with a variety of flow depths along their migrating corridors (in contrast to more technical fish passes, e.g. VSF, where the flow depth is typically mostly constant within a pool). Also, the proposed geometry is without unconnected crevices that can become ecological traps, as pointed out by (Plesiński et al., 2018). Although it was not an object of the present study, a

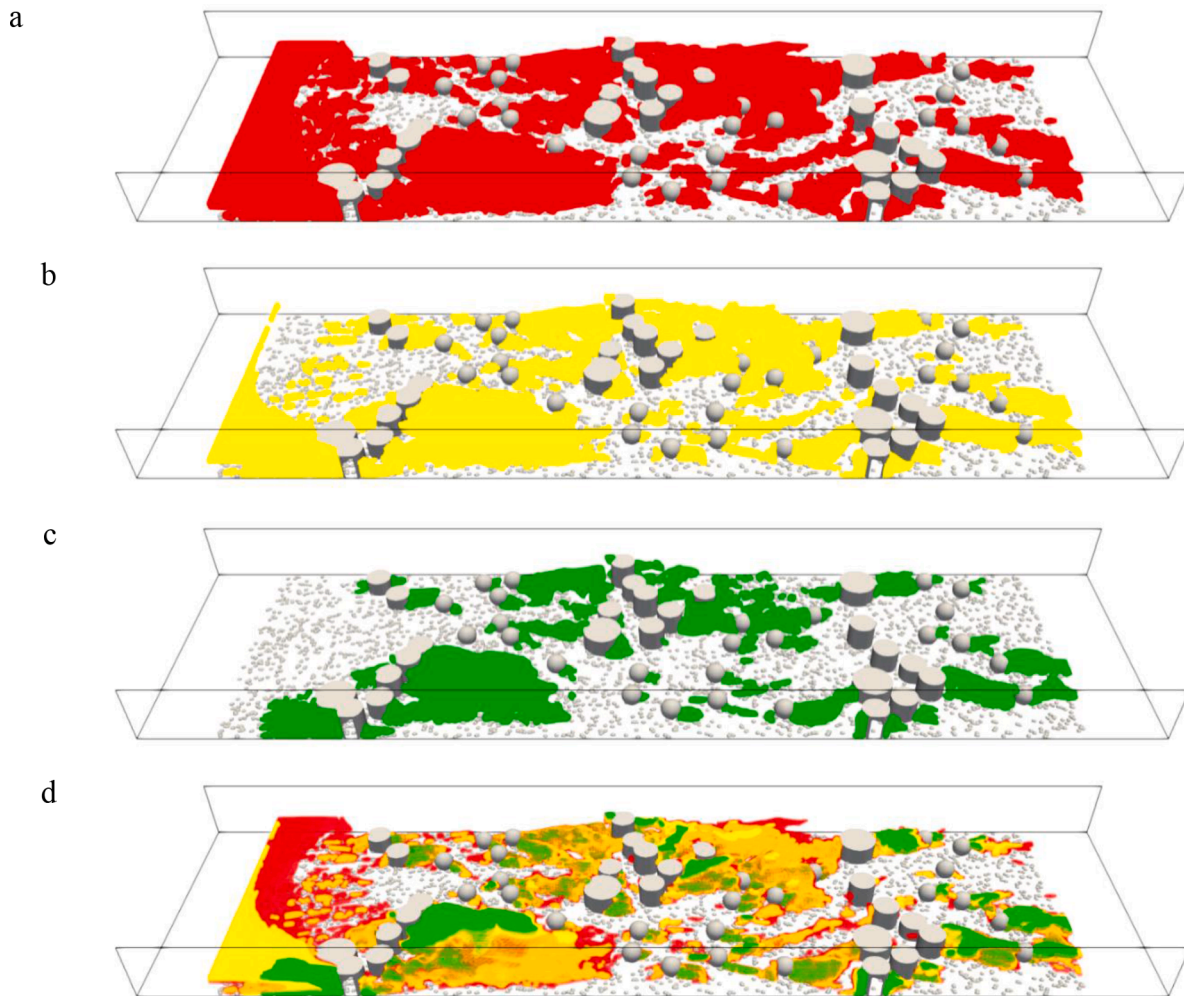


Fig. 11. Side view of migration zones with diameter $d \geq 0.03$ m, length $l \geq 0.15$ m for Q3 case: (a) limit zones, (b) effort zones, (c) rest zones, (d) all zones with some transparency to show the transition between the zones.

favorable tailwater effect could occur at the downstream end of the study site, increasing the downstream depth and decreasing the velocities, thus contributing to more suitable depths and velocity fields along the whole observed section.

Based on resulting velocity fields (Fig. 9), the proposed geometry provides suitable conditions for all target species: the weakest swimmers can find their way upstream staying close to the bottom, while better swimmers can overcome even the localized areas of larger velocities. The fact that velocity fields parallel to the bed change with their distance from the bed is an important advantage in comparison to more technical fish passes, where flow fields are much more uniform (e.g. in a VSF they are depth-averaged and flow patterns remain practically the same in all pools).

Diverse velocity fields are also favorable in terms of whirls, as pointed out by (Puzdrowska and Heese, 2019). The size of vortices depends on the size of the flow (e.g. distances between the obstacles), thus the proposed geometry does not allow the formation of potentially problematic larger whirls. At the same time, the configuration is not too uniformly fragmented, thus avoiding the disadvantages of the technical solutions such as baffled chutes (Bylak et al., 2017).

Based on calculated migration routes, resting areas, and their mutual distance (Figs. 10, 11, 12), the proposed geometry provides the fish with ample resting space to recover their strength after periods of burst and/or critical swimming sessions. The velocity fields and migration zones show localized regions of higher flow velocities and thus fragmented migration routes during higher discharge, indicating that the weaker

swimmers might not be able to migrate in these conditions. However, the distances between migration zones (Fig. 12) are small enough for the stronger swimmers to easily cross areas of faster flow, as they can maintain various levels of swimming effort for long enough. Comparing these results against the swimming capacities of target species, it is clear that all species, except the lamprey, should be able to migrate even during the high discharge period. However, most fish species do not migrate during high discharge periods, and such periods occur rarely and have limited duration, so they should not be taken as a reference, but rather as the limit conditions.

The present study could be upgraded with simulations of movable bed elements to investigate how the ramp and its flow characteristics would change due to sediment transport. Such simulations would be a valuable contribution to evaluations of restoration projects, e.g. like the one described in (Mikuš et al., 2021).

5. Conclusions

Several stages of fish ramp geometry optimization were performed, including variants of channel slope, bed roughness, and sizes and positions of flow diverting obstacles. Adjusting the geometry to the characteristics of the actual site led to a near-natural ramp configuration that provides flow conditions diverse enough to allow different fish species to find their preferred migration route. The flow conditions were presented in terms of velocity fields at selected planes parallel to the channel bed. Based on the fish swimming performance criteria, suitable migration

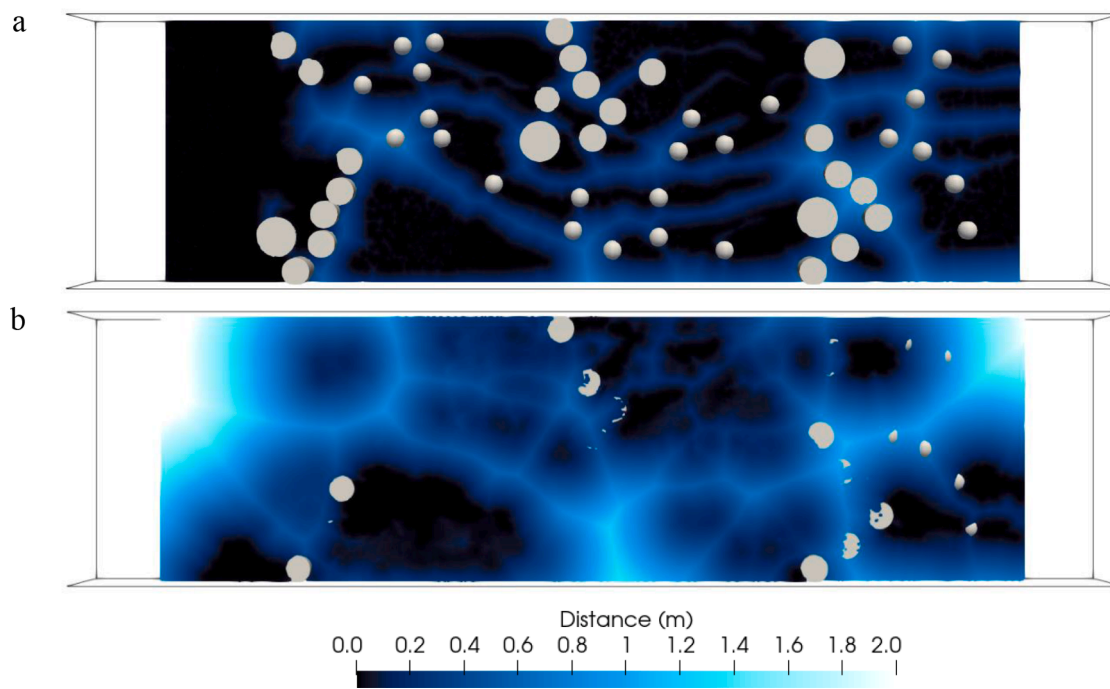


Fig. 12. Plan view of distances to effort zones [m]: a) for Q1 case, b) for Q3 case.

Table 6

Summary of migration zones characteristics.

case	total fluid volume [m ³]	zone size $r_m \geq 0.03$ m, $l_m \geq 0.15$ m		effort zone $u_m \leq 0.45$ m/s		limit zone $u_m \leq 0.52$ m/s	
		rest zone $u_m \leq 0.34$ m/s volume [%]	mean \bar{v} [m/s]	volume [%]	mean \bar{v} [m/s]	volume [%]	mean \bar{v} [m/s]
Q1	5.54	38.7	0.19	58.3	0.25	66.4	0.28
Q3	16.01	9.3	0.22	18.0	0.30	25.9	0.35

routes were identified. These routes form complex 3D structures made of numerous volumes of slower fluid and give important insights into a future design of similar eco-hydraulics applications. These representations also indicate how fish might perceive the river, identifying areas of favorable and unfavorable spaces to navigate the rivers.

The presented analysis of flow over a complex geometry confirms that the design of a nature-like fish pass configuration can be optimized using a fully 3D numerical model based on the SPH method. The resulting flow can be analyzed in great detail, allowing calculations of fluid depths, velocity fields, flow area – flow velocity ratio, migration zones, and their mutual distances. This means the decision makers can now get better insight into the flow features that were previously difficult to quantify, leading to more efficient designs of fish passages.

In terms of software development, improvements to the validated and verified DualSPHysics model were implemented to achieve the objectives of the present study. A new tool named FlowRest was devised to allow a detailed quantification of migration zones.

Future work will focus on importing additional non-uniformly shaped 3D objects into the model to mimic natural stones and rocks. The riverbed slope will be diversified to accommodate the natural riffle-pool sequence characteristics. Furthermore, an improved tool for the quantification of trajectories (focused on whirls) will be applied, enabling complex fishway flows to be analyzed in even more detail. Finally, with the employment of a multi-phase combination of water and sediment, the simulations will produce even more realistic results, allowing investigations of sediment transport in stream restoration solutions.

CRediT authorship contribution statement

Gorazd Novak: Conceptualization, Formal analysis, Investigation, Data curation, Writing – original draft. **Polona Pengal:** Conceptualization, Investigation, Writing – original draft. **Ana T. Silva:** Conceptualization, Writing – original draft. **José M. Domínguez:** Data curation, Methodology, Software, Visualization, Writing – review & editing. **Angelo Tafuni:** Methodology, Software, Visualization, Writing – review & editing. **Matjaž Četina:** Funding acquisition, Supervision, Writing – review & editing. **Dušan Žagar:** Funding acquisition, Supervision, Writing – review & editing.

Declaration of Competing Interest

The authors declare that they have no known competing financial interests or personal relationships that could have appeared to influence the work reported in this paper.

Data availability

Data will be made available on request.

Acknowledgements

This work was partially funded by the Slovenian Research Agency (ARRS) as part of the research programme P2-0180 »Water Science and Technology, and Geotechnical Engineering: Tools and Methods for Process Analyses and Simulations, and Development of Technologies«.

This work was partially supported by the project SURVIWEC PID2020-113245RB-I00 financed by MCIN/AEI/10.13039/501100011033 and by the project ED431C 2021/44 "Programa de Consolidación e Estructuración de Unidades de Investigación Competitivas" financed by Xunta de Galicia, Consellería de Cultura, Educación e Universidade. This study forms part of the Marine Science programme (ThinkInAzul) supported by Ministerio de Ciencia e Innovación and Xunta de Galicia with funding from European Union NextGenerationEU (PRTR-C17.11) and European Maritime and Fisheries Fund.

References

- Aarestrup, K., Økland, F., Hansen, M.M., Righton, D., Gargan, P., Castonguay, M., Bernatchez, L., Howey, P., Sparholt, H., Pedersen, M.I., McKinley, R.S., 2009. Oceanic spawning migration of the European eel (*anguilla anguilla*). *Science* 325, 1660. <https://doi.org/10.1126/science.1178120>.
- Altomare, C., Crespo, A.J.C., Domínguez, J.M., Gómez-Gesteira, M., Suzuki, T., Verwaest, T., 2015. Applicability of Smoothed Particle Hydrodynamics for estimation of sea wave impact on coastal structures. *Coast. Eng.* 96, 1–12. <https://doi.org/10.1016/j.coastaleng.2014.11.001>.
- Baki, A.B.M., Zhu, D.Z., Harwood, A., Lewis, A., Healey, K., 2020. Hydraulic design aspects of rock-weir fishways with notch for habitat connectivity. *J. Ecohydraulics* 5, 94–109. <https://doi.org/10.1080/24705357.2019.1652706>.
- Baudoin, J.M., Burgun, V., Chanseau, M., Larinier, M., Ovidio, M., Sremski, W., Steinbach, P., Voegtle, B., 2015. Assessing the passage of obstacles by fish. Belletti, B., García de Leaniz, C., Jones, J., Bizzi, S., Börger, L., Segura, G., Castelletti, A., van de Bund, W., Aarestrup, K., Barry, J., Belka, K., Berkhuyzen, A., Birnie-Gauvin, K., Bussetini, M., Carolli, M., Consuegra, S., Dopico, E., Feierfeil, T., Fernández, S., Fernandez Garrido, P., Garcia-Vazquez, E., Garrido, S., Giannico, G., Gough, P., Jepsen, N., Jones, P.E., Kemp, P., Kerr, J., King, J., Łapińska, M., Lázaro, G., Lucas, M.C., Marcello, L., Martin, P., McGinnity, P., O’Hanley, J., Olivo del Amo, R., Parasiewicz, P., Pusch, M., Rincon, G., Rodriguez, C., Royte, J., Schneider, C.T., Tummers, J.S., Vallesi, S., Vowles, A., Verspoor, E., Wanningen, H., Wautzen, K.M., Wildman, L., Zalewski, M., 2020. More than one million barriers fragment Europe’s rivers. *Nature* 588, 436–441. <https://doi.org/10.1038/s41586-020-3005-2>.
- Birnie-Gauvin, K., Franklin, P., Wilkes, M., Aarestrup, K., 2019. Moving beyond fitting fish into equations: Progressing the fish passage debate in the Anthropocene. *Aquat. Conserv. Mar. Freshw. Ecosyst.* 29, 1095–1105. <https://doi.org/10.1002/aqc.2946>.
- Bylak, A., Kukuła, K., Plesiński, K., Radecki-Pawlik, A., 2017. Effect of a baffled chute on stream habitat conditions and biological communities. *Ecol. Eng.* 106, 263–272. <https://doi.org/10.1016/J.ECOLENG.2017.05.049>.
- Chamberlain, L., 2020. Death by a thousand cuts Black catalogue of small hydropower plants.
- Crespo, A.J.C., Gómez-Gesteira, M., Dalrymple, R.A., 2007. Boundary conditions generated by dynamic particles in SPH methods. *Comput. Mater. Contin.* 5, 173–184. <https://doi.org/10.3970/cmc.2007.005.173>.
- Deinet, S., Scott-Gatty, K., Rotton, H., Twardek, W. M., Marconi, V., McRae, L., Baumgartner, L. J., Brink, K., Clausen, J. E., Cooke, S. J., Darwall, W., Eriksson, B. K., García de Leaniz, C., Hogan, Z., Royte, J., Silva, L. G. M., Thieme, M. L., Tickne, O.L.F., 2020. The Living Planet Index for Migratory Freshwater Fish - Technical Report 131–149.
- Dingle, H., Alistair Drake, V., 2007. What is migration? *Bioscience* 57, 113–121. <https://doi.org/10.1641/B570206>.
- Domínguez, J.M., Fourtakas, G., Altomare, C., Canelas, R.B., Tafuni, A., García-Feal, O., Martínez-Estévez, I., Mocos, A., Vacondio, R., Crespo, A.J.C., Rogers, B.D., Stansby, P.K., Gómez-Gesteira, M., 2022. DualSPHysics: from fluid dynamics to multiphysics problems 9, 867–895. <https://doi.org/10.1007/s40571-021-00404-2>.
- EEA European Environment Agency, 2018. European waters - assessment of status and pressures 2018. EEA Report No 7/2018.
- English, A., Domínguez, J.M., Vacondio, R., Crespo, A.J.C., Stansby, P.K., Lind, S.J., Chiapponi, L., Gómez-Gesteira, M., 2022. Modified dynamic boundary conditions (mDBC) for general-purpose smoothed particle hydrodynamics (SPH): application to tank sloshing, dam break and fish pass problems 9, 911–925. <https://doi.org/10.1007/s40571-021-00403-3>.
- European Commission, 2020. Communication from the Commission to the European Parliament, the Council, the European Economic and Social Committee and the Committee of the Regions. *EU Biodiversity Strategy for 2030*. European Commission.
- European Commission, 2019. The European Green Deal. *Eur. Comm.* 53, 24. <https://doi.org/10.1017/CBO9781107415324.004>.
- European Environment Agency, 2020. Tracking barriers and their impacts on European river ecosystems. *Brief. 30/2020 - Water Mar. Environ.* 1–9.
- FAO & DVWK, 2002. Fish Passes - design, dimensions and monitoring.
- Fourtakas, G., Domínguez, J.M., Vacondio, R., Rogers, B.D., 2019. Local uniform stencil (LUST) boundary condition for arbitrary 3-D boundaries in parallel smoothed particle hydrodynamics (SPH) models. *Comput. Fluids* 190, 346–361. <https://doi.org/10.1016/j.compfluid.2019.06.009>.
- Fuentes-Pérez, J.F., Silva, A.T., Tuhtan, J.A., García-Vega, A., Carbonell-Baeza, R., Musall, M., Kruusmaa, M., 2018. 3D modelling of non-uniform and turbulent flow in vertical slot fishways. *Environ. Model. Softw.* 99, 156–169. <https://doi.org/10.1016/J.ENVSOF.2017.09.011>.
- Gough, P., Fernandez Garrido, P., Van Herk, J., 2018. Dam Removal. A viable solution for the future of our European rivers. *Dam Removal Europe*.
- Grinnell, J., 1917. The Niche-Relationships of the California Thrasher Author (s): Joseph Grinnell Published by : Oxford University Press Stable URL : <https://www.jstor.org/stable/4072271>. *Auk* 34, 427–433.
- Hutchinson, G.E., 1957. Concluding remarks. *Cold Spring Harb. Symp. Quant. Biol.* 22, 415–427.
- IUCN, 2020. IUCN Global Standard for Nature-based Solutions. First edition 1–22.
- Jungwirth, M., 1998. River Continuum and Fish Migration - Going Beyond the Longitudinal River Corridor in Understanding Ecological Integrity. *Fish Migration and Fish Bypasses*. Fishing News Books, pp. 19–32.
- Kupferschmidt, C., Zhu, D.Z., 2017. Physical modelling of pool and weir fishways with rock weirs. *River Res. Appl.* 33, 1130–1142. <https://doi.org/10.1002/rra.3157>.
- Liermann, C.R., Nilsson, C., Robertson, J., Ng, R.Y., 2012. Implications of dam obstruction for global freshwater fish diversity. *Bioscience* 62, 539–548. <https://doi.org/10.1525/bio.2012.62.6.5>.
- Lucas, M.C., Baras, E., Thom, T.J., Duncan, A., Slavik, O., 2001. Migration of Freshwater Fishes. Blackwell Science Ltd. <https://doi.org/10.1002/9780470999653>.
- Mader, H., Unfer, G., Schmutz, S., 1998. The Effectiveness of Nature-like Bypass Channels in a Lowland River, the Marchfeldkanal. In: Jungwirth, M., Schmutz, S., Weiss, S. (Eds.), *Fish Migration and Fish Bypasses*. Fishing News Books, pp. 384–402.
- Marti-Puig, P., Serra-Serra, M., Campos-Candela, A., Reig-Bolano, R., Manjabacas, A., Palmer, M., 2018. Quantitatively scoring behavior from video-recorded, long-lasting fish trajectories. *Environ. Model. Softw.* 106, 68–76. <https://doi.org/10.1016/J.ENVSOF.2018.01.007>.
- Mikuš, P., Wyzga, B., Bylak, A., Kukuła, K., Liro, M., Oglecki, P., Radecki-Pawlik, A., 2021. Impact of the restoration of an incised mountain stream on habitats, aquatic fauna and ecological stream quality. *Ecol. Eng.* 170. <https://doi.org/10.1016/J.ECOLENG.2021.106365>.
- Monaghan, J.J., Gingold, R.A., 1983. Shock simulation by the particle method SPH. *J. Comput. Phys.* 52, 374–389. [https://doi.org/10.1016/0021-9991\(83\)90036-0](https://doi.org/10.1016/0021-9991(83)90036-0).
- Nichols, C., Smith, A., Huelsman, S., Schemmel, C., Doll, J.C., Jacquemin, S.J., 2018. Preliminary understanding of complexities in swimming performance of common minnow (Cyprinidae) taxa. *Ohio J. Sci.* 118, 16–24. <https://doi.org/10.18061/OJS.V118I2.6117>.
- Northcote, T.G., 1978. Migratory strategies and production in freshwater fishes. In: Gerking, S.D. (Ed.), *Ecology of Freshwater Fish Production*. Blackwell Science. Oxford, pp. 326–359.
- Novak, G., Domínguez, J.M., Tafuni, A., Silva, A.T., Pengal, P., Četina, M., Žagar, D., 2021. 3-D Numerical Study of a Bottom Ramp Fish Passage Using Smoothed Particle Hydrodynamics. *Water*. <https://doi.org/10.3390/w13111595>.
- Novak, G., Tafuni, A., Domínguez, J.M., Četina, M., Žagar, D., 2019. A numerical study of fluid flow in a vertical slot fishway with the smoothed particle hydrodynamics method. *Water*. <https://doi.org/10.3390/w11091928>.
- Pengal, et al., 2021. Razdrobljenost rek v Sloveniji. In: Cerkenik, S. (Ed.), *Zbornik Referatov Simpozija Vodni Dnevi 2021 z Mednarodno Udeležbo (in Slovenian)*. Slovensko društvo za zaščito voda.
- Plesiński, K., Bylak, A., Radecki-Pawlik, A., Mikołajczyk, T., Kukuła, K., 2018. Possibilities of fish passage through the block ramp: model-based estimation of permeability. *Sci. Total Environ.* 631–632, 1201–1211. <https://doi.org/10.1016/J.SCIOTENV.2018.03.128>.
- Puzdrowska, M., Heese, T., 2019. Experimental studies on the spatial structure and distribution of flow velocities in bolt fishways. *J. Ecol. Eng.* 20, 82–99. <https://doi.org/10.12911/22998993/113044>.
- Radinger, J., Wolter, C., 2014. Patterns and predictors of fish dispersal in rivers. *Fish Fish* 15, 456–473. <https://doi.org/10.1111/faf.12028>.
- Raymond, C.M., Pam, B., Breil, M., Nita, M.R., Kabisch, N., de Bel, M., Enzi, V., Frantzeskaki, N., Geneletti, D., Cardinaletti, M., Lovinger, L., Basnou, C., Monteiro, A., Robrecht, H., Sgrigna, G., Munari, L., Callapietra, C., 2017. An Impact Evaluation Framework to Support Planning and Evaluation of Nature-based Solutions Projects, EKLIPSE Expert Working Group report.
- Schmutz, S., Mielach, C., 2013. Measures for ensuring fish migration at transversal structures 1–52.
- Shim, T., Kim, Z., Seo, D., Kim, Y.O., Hwang, S.J., Jung, J., 2020. Integrating hydraulic and physiologic factors to develop an ecological habitat suitability model. *Environ. Model. Softw.* 131. <https://doi.org/10.1016/J.ENVSOF.2020.104760>.
- Silva, A.T., Lucas, M.C., Castro-Santos, T., Katopodis, C., Baumgartner, L.J., Thieme, J.D., Aarestrup, K., Pompeu, P.S., O’Brien, G.C., Braun, D.C., Burnett, N.J., Zhu, D.Z., Fjeldstad, H.P., Forseth, T., Rajaratnam, N., Williams, J.G., Cooke, S.J., 2018. The future of fish passage science, engineering, and practice. *Fish Fish* 19, 340–362. <https://doi.org/10.1111/faf.12258>.
- Sutphin, Z.A., Hueth, C.D., 2010. Swimming performance of larval pacific lamprey (*lampetra tridentata*). *Northwest Sci* 84, 196–200. <https://doi.org/10.3955/046.084.0209>.
- Tafuni, A., Domínguez, J.M., Vacondio, R., Crespo, A.J.C., 2018. A versatile algorithm for the treatment of open boundary conditions in Smoothed particle hydrodynamics GPU models. *Comput. Methods Appl. Mech. Eng.* 342, 604–624. <https://doi.org/10.1016/j.cma.2018.08.004>.
- Tudorache, C., Viaene, P., Blust, R., Vereecken, H., De Boeck, G., 2008. A comparison of swimming capacity and energy use in seven European freshwater fish species. *Ecol. Freshw. Fish* 17, 284–291. <https://doi.org/10.1111/j.1600-0633.2007.00280.x>.
- UNEP and FAO, 2020. The UN Decade on Ecosystem Restoration: Strategy 48.
- WWF, 2018. Living Planet Report - 2018: Aiming higher., Environmental Conservation.